Available online at www.sciencedirect.com
SCIENCE DIRECT®
Journal of Nuclear Materials 347 (2005) 94–103
journal of nuclear materials
www.elsevier.com/locate/jnucmat

Engineering product storage under the advanced fuel cycle initiative. Part I: An iterative thermal transport modeling scheme for high-heat-generating radioactive storage forms ☆,☆☆

Michael D. Kaminski *

Chemical Engineering Division, Argonne National Laboratory, 9700 South Cass Avenue, Argonne, IL 60439, USA

Received 9 March 2005; accepted 21 July 2005

Abstract

The US Department of Energy is developing an integrated nuclear fuel cycle technology under its Advanced Fuel Cycle Initiative (AFCI). Under the AFCI, waste minimization is stressed. Engineered product storage materials will be required to store concentrated radioactive cesium, strontium, americium, and curium for periods of tens to hundreds of years. The fabrication of such engineered products has some precedence but the concept is largely novel. We thus present a theoretical model used to calculate the maximum radial dimensions of right cylinder storage forms under several scenarios. Maximum dimensions are small, comparable to nuclear fuel pins in some cases, to avoid centerline melting temperatures; this highlights the need for a careful strategy for engineered product storage fabrication and storage.

PACS: 28.41.Kw

1. Introduction

The US Department of Energy is developing an integrated nuclear fuel cycle technology under its Advanced Fuel Cycle Initiative (AFCI) [1]. Under the AFCI, waste minimization is stressed. Burned UO_2 fuel will undergo extensive processing to (1) recycle fissionable material for continued burning in-reactor, (2) recover long-lived radionuclides for transmutation in transmutation reactors being designed under AFCI, (3) isolate high-specific-activity cesium and strontium isotopes for decay storage in monitored low-level storage facilities, and (4) stabilization of the much-reduced volume of waste material designated for geological disposal within the Yucca

☆ Work supported by the US Department of Energy, DOE/NE Nuclear Energy, Science and Technology, under Contract W-31-109-Eng-38.

* Tel.: +1 630 252 4777; fax: +1 630 252 5246.
E-mail address: kaminski@cmt.anl.gov

0022-3115/$ - see front matter © 2005 Published by Elsevier B.V.
doi:10.1016/j.jnucmat.2005.07.011

Mountain underground repository. As part of the processing scheme, americium and curium will be separated from the dissolved fuel, converted to solid form, and stored for a short period of time (10–50 years) until burned in the transmutation reactors. However, these elements generate tremendous amounts of heat due primarily to ^{241}Am ($T_{1/2} = 432$ years) and ^{244}Cm ($T_{1/2} = 18.1$ years) alpha decay products ($E_\alpha = 5.49$ MeV and 5.80 MeV primarily, respectively). Similarly, cesium and strontium isotopes will require solidification and stabilization for prolonged decay storage of 300–500 years. Cesium and strontium also have high-specific-activity from their decay (^{137}Cs $E_\beta = 0.514$ MeV; ^{90}Sr $E_\beta = 0.546$ MeV) and the decay of their short-lived daughter products (^{137m}Ba $E_\gamma = 0.662$ MeV; ^{90}Y $E_\beta = 2.28$ MeV). Because of the unique endpoint of these radionuclides under the AFCI, i.e., stable storage materials for future disposal or processing, they will have much different fabrication criteria than waste forms, actinide fuels, or transmutation targets under investigation by the Japanese, French, or US programs. Therefore, an important part of the AFCI program is determining the optimum methods for decay storage of cesium, strontium, americium, and curium.

The final separation scheme has not been determined, although the general consensus is that the separation process will produce a combined cesium and strontium product stream. It is still unclear whether americium and curium will be combined or separated into individual streams. Therefore, our analysis considers these options:

1. Separation of cesium and strontium in a combined stream.
2. Separation of americium and curium in a combined stream.
3. Separation of curium from americium and storage of curium (americium will exist in a combined TRU stream and will not be considered as a separate stream in this analysis).

We do not account for the possibility that Rb and Ba fission products will be separated along with the Cs and Sr. The implications of a Rb/Ba/Cs/Sr product are significant increases in total mass requiring storage, decreases in specific heat output, and potential effects on storage material stability. Calculations show that the storage form dimensions quoted in this paper can increase by 50% when the cesium and strontium are diluted with rubidium and barium. Importantly, we do not consider consequences of storage canister pressurization that may result from radiolysis or will occur from helium buildup.

As a first step toward engineered product storage development, we describe here a thermal transport model to establish the maximum storage form dimensions for individual storage containers under the scenarios described above. The model algorithm was developed by combining Fourier's Heat Conduction equations with Newton's Law of Cooling while modifying key parameters to account for porosity, solid phase mixtures, and finned surfaces. We consider storage in pure form and diluted in a stabilized matrix, and storage in a dry and wet storage facility. Our results show that even with the prodigious heat that is generated, the storage form radii for Am/Cm oxides are slightly larger than current specifications for light water reactor UO_2 fuel and mixed-oxide fuel fabrication. Radii for Cs/Sr oxides are larger. Under a diluted-storage-form scenario, we can increase the maximum radius by adjusting the radioactive load in the storage form and thereby tailor the durability of the storage form for long-term decay. Materials such as alumino-silicates and borosilicate glass for Cs/Sr, and Zircaloy and uranium dioxide for Am/Cm are investigated.

2. Algorithm description

2.1. Isotropic volumetric heat source

The heat source was calculated from the decay mode of the individual radionuclides by converting the decay energy into a thermal energy, assuming a fractional deposition of the decay particle in the storage form. For alpha and beta decay we assumed 100% of the energy was deposited[1] in the storage form since the average path length of 1-MeV alpha particles in solids is several micrometers and the path length for 1-MeV beta particles is several millimeters. Rigorously, the heat is

$$q[W] = \frac{0.693}{T_{1/2}} N(t) \times 1.6 \times 10^{-13} \times \left(\sum_i f_i^\gamma E_i^\gamma y_i^\gamma + \sum_j f_j^\beta E_j^\beta y_j^\beta + \sum_k f_k^\alpha E_k^\alpha y_k^\alpha \right), \quad (1)$$

where $T_{1/2}$ = the half-life of the radionuclide in seconds, $N(t)$ = the number of atoms of the radionuclide at time t, 1.6×10^{-13} = the units conversion factor (J/keV), f = the fraction of energy deposited in the waste form (0.33 for gamma, 1 for beta and alpha)), $E_{i,j}$ = the kinetic energy carried by the radiation in keV, and $y_{i,j,k}$ = the decay mode yield for a particular decay of the ith gamma ray, jth beta ray, kth alpha particle.

[1] The average beta energy was assumed to be 1/3 the maximum energy due to neutrino emission.

2.2. Governing heat transport equations

The general equation for heat transport in a right, cylindrical storage form (Fig. 1) is

$$\frac{\partial T}{\partial r^2}+\frac{1}{r}\frac{\partial T}{\partial r}+\frac{1}{r^2}\frac{\partial^2 T}{\partial \phi^2}+\frac{\partial^2 T}{\partial z^2}+\frac{g(r,t)}{k}=\frac{1}{\alpha}\frac{\partial T}{\partial t}. \tag{2}$$

For long cylinders (ignoring z-axis transport), isotropic heat conduction (no azimuthal ϕ dependence), and a homogeneous heat source at steady state ($g(r, t) = g_0$, $\delta T/\delta t = 0$), we reduce the equation to

$$\frac{\mathrm{d}T}{\mathrm{d}r^2}+\frac{1}{r}\frac{\mathrm{d}T}{\mathrm{d}r}+\frac{g_0}{k}=0, \tag{3}$$

with the general solution

$$T(r)=\frac{-g_0 r^2}{4k}+C_1\ln r+C_2. \tag{4}$$

The boundary condition in the heated storage form is the Neumann type. At $r = 0$,

$$\left.\frac{\mathrm{d}T}{\mathrm{d}r}\right|_{r=0}=0, \tag{5}$$

but at the radioactive-material (*rad*) canister (*can*) interface we have the convective boundary conditions at an imperfect interface, or

$$-k_{\mathrm{rad}}\left.\frac{\mathrm{d}T}{\mathrm{d}r}\right|_i=h_{\mathrm{c}}(T_i-T_{i+\Delta})=-k_{\mathrm{can}}\left.\frac{\mathrm{d}T}{\mathrm{d}r}\right|_{i+\Delta}. \tag{6}$$

For the canister, the inner surface is as above and the outer surface boundary condition is the second kind, the convective boundary condition to a bulk coolant

$$T_{\mathrm{surface}}=T_{\mathrm{bulk}}+\frac{g_0}{h_{\mathrm{fluid}}A}. \tag{7}$$

The radial temperature profile within the radioactive material is then given by

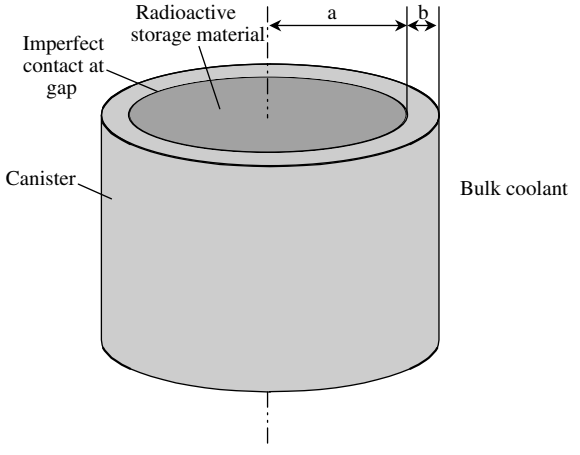

Fig. 1. Schematic of right, cylindrical storage form.

$$T_{\mathrm{rad}}(r)=T_{\mathrm{centerline}}-\frac{q'}{4\pi k_{\mathrm{rad}}}\left(\frac{r^2}{a^2}\right), \tag{8}$$

where

$$q'=\frac{\pi d^2}{4}g_0. \tag{9}$$

The temperature at the radioactive material-gap interface $T_{\mathrm{rad\text{-}gap}}$ is

$$T_{\mathrm{rad\text{-}gap}}=\frac{q'}{2\pi h_{\mathrm{c}}a}+T_{\mathrm{gap\text{-}can}}, \tag{10}$$

the temperature at the gap-canister interface $T_{\mathrm{gap\text{-}can}}$ is

$$T_{\mathrm{gap\text{-}can}}=\frac{q'}{2\pi k_{\mathrm{can}}}\ln\left(\frac{a+b}{a}\right)+T_{\mathrm{surface}}, \tag{11}$$

and the resulting centerline maximum temperature is

$$T_{\mathrm{centerline}}=\frac{q'}{2\pi}\left[\frac{1}{2k_{\mathrm{rad}}}+\frac{1}{k_{\mathrm{can}}}\ln\left(\frac{a+b}{a}\right)+\frac{1}{ah_{\mathrm{c}}}+\frac{1}{h_{\mathrm{fluid}}(a+b)}\right]+T_{\mathrm{bulk}}. \tag{12}$$

2.3. Convective heat transfer coefficient

The model assumes that the storage facility will implement passive cooling methods so that natural convection is the governing mode. The convective heat transfer coefficient h_{conv} was derived via the Nusselt number Nu [2], which is a product of the Grashoff Gr and Prandtl number Pr. Our model uses the formulation for a long, horizontal pipe

$$Nu=0.518(GrPr)^{1/4}=\frac{h_{\mathrm{conv}}D}{k_{\mathrm{fluid}}} \tag{13}$$

for $10^4 < GrPr < 10^{12}$, where

$$Pr=\frac{C_p\mu_{\mathrm{fluid}}}{k_{\mathrm{fluid}}} \tag{14}$$

and $Pr = 0.7$ for air at the temperature range of interest (300–900 K) and $Pr = 1.7$ for water at 363 K,

$$Gr=\frac{D^3\rho_{\mathrm{fluid}}^2 g\beta_{\mathrm{f}}\Delta T}{\mu_{\mathrm{fluid}}^2}=\frac{D^3 g\beta_{\mathrm{f}}\Delta T}{\upsilon_{\mathrm{fluid}}^2}, \tag{15}$$

where the volumetric thermal expansion coefficient is

$$\beta_{\mathrm{f}}=\frac{-1}{\rho_{\mathrm{fluid}}}\left.\frac{\mathrm{d}\rho}{\mathrm{d}T}\right|_{\mathrm{film}} \tag{16}$$

but can be shown for an ideal gas to be

$$\frac{1}{T_{\mathrm{film}}}=\frac{1}{1/2(T_{\mathrm{surface}}+T_{\mathrm{bulk}})} \tag{17}$$

and

$$\Delta T=(T_{\mathrm{surface}}-T_{\mathrm{bulk}}). \tag{18}$$

The kinematic viscosity of air is

$$v_{air} = -1.1555 \times 10^{-14} T_{film}^3 + 9.5728 \times 10^{-11} T_{film}^2 + 3.7604 \times 10^{-8} T_{film} - 3.4484 \times 10^{-6} \quad (19)$$

and v_{water} is 2.90×10^{-7} m^2/s at 373 K.

It is likely that the engineered product storage forms will be stored vertically instead of horizontally; however, the correction between a horizontal form and a vertical form is small. Kato et al. [3] describe the following relation for vertical cylinders with $Gr < 10^9$:

$$Nu = 0.683(GrPr)^{1/4}\left(\frac{Pr}{0.861 + Pr}\right)^{1/4}. \quad (20)$$

A plot of Eqs. (13) and (20) (Fig. 2) shows that the two relations differ by less than 20% in water and 10% in air coolant.

2.4. Radiative heat transfer coefficient

The radiative heat transfer coefficient h_{rad} was calculated based on radiation from a long, horizontal cylinder into a completely absorbing medium [4] where the heat q is proportional to T^4 by

$$q = A_1 \varepsilon_1 \sigma (T_1^4 - T_2^4), \quad (21)$$

where A_1 is the surface area of the radiating cylinder, ε is the emissivity of the radiating surface material (0.7–1 for metals), and σ is the Stefan–Boltzmann constant (5.67×10^{-8} W/m^2/K^4). Combining this with the analogous expression using the Newton Law of Cooling methodology,

$$q = h_{rad} A_1 (T_1 - T_2), \quad (22)$$

we obtain

$$h_{rad} = \varepsilon_1 \sigma \frac{(T_1^4 - T_2^4)}{(T_1 - T_2)}. \quad (23)$$

The total heat transfer coefficient h_{fluid} from the storage form surface is given by adding the radiative and convective terms.

$$h_{fluid} = h_{conv} + h_{rad}. \quad (24)$$

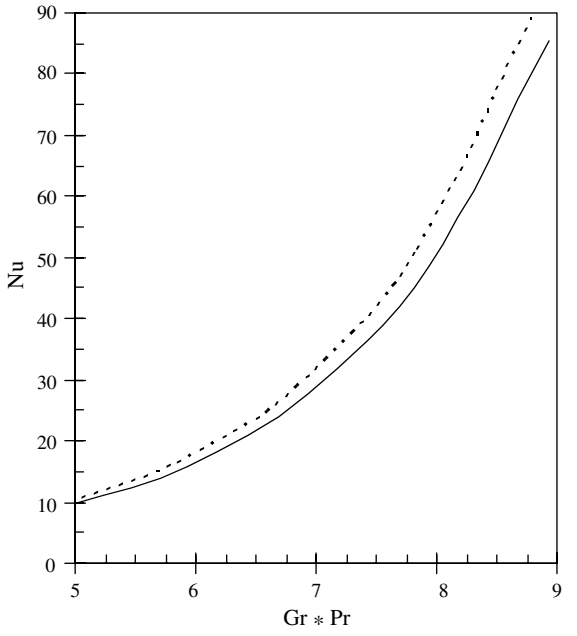

Fig. 2. Nusselt number calculated for long horizontal and vertical pipes for $Gr * Pr$ values typical for natural convection in air coolant.

2.5. Heat transfer coefficient for finned surfaces

The convective heat transfer coefficient can be enhanced by incorporating fins onto the surface. We modeled the effect of fins using the method of Kern [4]. The efficiency of the fin Ω is

$$\Omega = \frac{h_{b,conv}}{h_{f,conv}}, \quad (25)$$

where $h_{b,conv}$ is the convective heat transfer coefficient for the bare (unfinned) portion of the tube and $h_{f,conv}$ is the convective heat transfer coefficient for the finned surfaces of the tube. Ω is determined by finding the intersect of a family of curves representing the fin size (dimensionless) and heat transfer coefficient of the unfinned or bare surface. To this end we define the following:

r_b = radial distance from center of storage form to edge of bare cylinder,
r_e = radial distance from center of storage form to edge of fin,
h_{conv} = convective heat transfer coefficient of bare cylinder in fluid,
k_{fin} = thermal conductivity of fin/storage form,
y_b = half-thickness of fin,
A_{uf} = unfinned surface area of storage form,
A_f = finned surface area of storage area, and
h_{eff} = effective convective heat transfer coefficient based on inner tube radius.

In practice, one calculates the effective surface area A_{eff} of the finned cylinder from Ω as

$$A_{eff} = A_{uf} + \Omega A_f. \quad (26)$$

Then, the effective convective heat transfer coefficient for the finned cylinder is

$$A_{eff} \frac{h_f}{2\pi r_b H} = h_{eff}, \quad (27)$$

where H is the height of the cylinder assumed to be 10 times the diameter.

2.6. Effect of porosity on the thermal conductivity of the storage form

For solids less than theoretical density, k_{rad} is replaced by k_{porous}. The thermal conductivity of porous solids with a porosity ε, derived by Krupitzka [5], is

$$k_{porous} = k_{fluid}\left(\frac{k_{rad}}{k_{fluid}}\right)^{0.280-0.757\log\varepsilon-0.057\log\left(\frac{k_{rad}}{k_{fluid}}\right)} \quad \text{for } 0.2 \leqslant \varepsilon \leqslant 0.6, \tag{28}$$

where k_{fluid} is the k of the fluid filling the void space (we assume air).

2.7. Thermal conductivity of a mixture of material in the storage form

The thermal conductivity of a mixture composed of a major (subscript 1) and minor (subscript 2) phase is estimated by Benveniste [6] as

$$k_{mixture} = k_1\frac{2(1-v)+\beta\left[(1+2v)+2\frac{k_1}{k_2}(1-v)\right]}{2+v+\beta\left[(1-v)+\frac{k_1}{k_2}(2+v)\right]} \quad \text{for } v \leqslant \pi/6, \tag{29}$$

where v is the fraction of the minor phase. The term β is

$$\beta = \frac{r_2}{k_1 R_k}, \tag{30}$$

where r_2 is the radius of spherical particles representing the minor phase, and R_k is the Kapitza resistance defined in terms of the convective heat transfer coefficient (called the Kapitza conductance, h_{12}) at the interface between major phase 1 and minor phase 2 or

$$R_k = \frac{1}{h_{12}}, \tag{31}$$

where $h_{12} = 1.67\times10^7$ W/m^2/K for diamond in a ZnS matrix [7]. It is worthy to note that $k_{mixture}$ is not a particularly sensitive function of h_{12} for h_{12} on the order of 10^7 W/m^2/K. In addition, in the range of minor phase concentration (<15%) $k_{mixture}$ is not a sensitive function of the particle size of the minor phase (Fig. 3). For k_1 and k_2 we use the theoretically dense values for the thermal conductivity. If the mixture is less than theoretical density then the resulting $k_{mixture}$ replaces k_{solid} in Eq. (27) to determine the k for the porous mixture.

2.8. Model construction and iteration

The combined equations described in the Methods section were input into a Microsoft® Excel spreadsheet as an algorithm that requires user iteration to produce a unique solution to the temperature profile within the cylindrical storage form. The centerline temperature is determined by invoking Eq. (12). $k_{rad} = k_{porous}$ is from Eq. (28) for porous solids or Eqs. (28) and (29) for porous mixtures. The fluid filling the pore space is air ($k = 0.04$ W/m/K @ 500 K). h_{fluid} is from Eq. (22) and suitably modified in Eq. (25) for finned surfaces. A stainless steel canister is assumed, with a wall thickness of $b = 0.005$ m. The convective heat transfer coefficient for the gap h_c is fixed at 1000 W/m^2/K. The bulk fluid temperature is fixed at 363 K for air coolant and 313 K for water coolant. Additional parameters needed for this analysis are given below

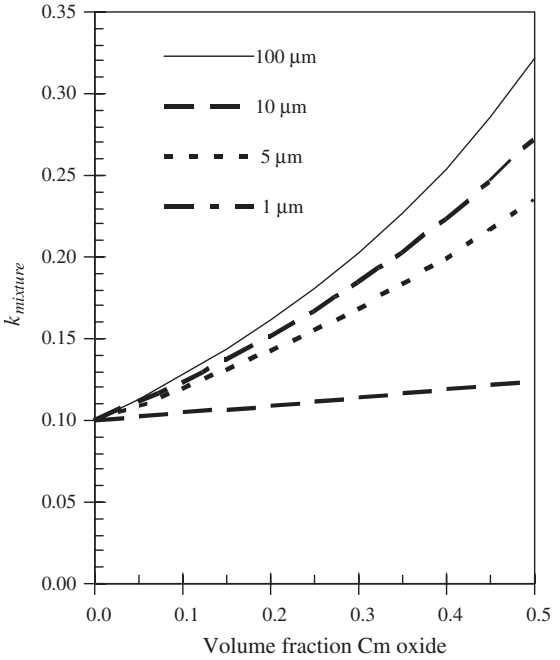

Fig. 3. Plot of $k_{mixture}$ versus v for a mixture of Am_2O_3 and Cm_2O_3 ($k_{Am\,oxide} = 0.1$ W/m/K and $k_{Cm\,oxide} = 2$ W/m/K, $h_{12} = 1.67\times10^7$ W/m^2/K).

Kapitza resistance	5.99×10^{-6} m^2 K/W
Radius of the particulate in the minor phase	5.0×10^{-6} m
Emissivity of steel canister	0.9
Kinematic viscosity of water	2.90×10^{-7} m^2/s
Coefficient of thermal expansion for water	6.54×10^{-4} @ 80 °C
Kinematic viscosity of air	1.79×10^{-5} m^2/s
Specific power for Am/Cm oxide	0.29 W/g
Specific power of Cs/Sr oxide	0.18 W/g

The thermal conductivity and density for some materials are given in Table 1.

Table 1
Thermal conductivities W/m/K (and densities g/cm^3) at operating temperatures typical of storage forms

Radioactive material, k (and ρ)		Non-radioactive material, k (and ρ)	
UO_2	5.19 (10.7)	Zircaloy	26.0 (6.5)
Am	10	Zirconia	2.5 (5.9)
Am_2O_3	0.10 (11.7)	Borosilicate glasses	0.5–1
Cm	10	Steel 304	22
Cm_2O_3	2.0 (12.7)	Aluminum	300 (2.7–2.8)
CsCl	0.9	Al-silicates (mullite)	4.0
Cs_2O	0.9 (4.6)	Air (373 K)	0.0346 (1.17×10^{-3})
Sr	35	Air (500 K)	0.04
SrO	9.0 (5.1)	Stainless steel (700 K)	22 (8.0)
89.5% Am_2O_3/10.5% Cm_2O_3	0.12 (11.8)	He (500 K)	0.22
74% Cs_2O/26% SrO	1.02 (4.8)	Water	0.6923

After the user inputs the properties of the storage form, the user guesses at a and h_{fluid} and the program calculates the new h_{fluid} by Eq. (24) and the centerline temperature. This iteration continues until several criteria are met:

- If the coolant is water, the surface temperature of the canister cannot exceed 90 °C to avoid nucleate boiling or the centerline temperature is equal to 90% of the absolute melting temperature or stable temperature,[2] indicating the maximum radial dimension of the storage form.
- The calculated total heat transfer coefficient h_{fluid} matches the guessed value for the total heat transfer coefficient.
- $Gr\,Pr < 10^{12}$.

The iteration is facilitated with Microsoft® Excel Solver. Using Solver, the difference between the user input value for the total heat transfer coefficient and the calculated heat transfer coefficient is minimized by modifying the cells containing the value for a and h_{fluid} under the constraints that the centerline temperature is equal to 90% of the melting temperature, the $r_{\text{rad}} > 0$, and $h_{\text{fluid}} > 0$, which ensures a unique solution.

3. Results

Using the model developed here, we calculated the maximum radii for storage forms consisting of the radioactive material in a stainless steel canister. The analysis conditions describe storage of individual canisters in a vault or pool where natural convection cools the canisters and the fluid (air or water) inlet temperature is constant. Vertical and horizontal storage of the canisters is described. All values for storage-form radii are given for the radioactive storage material and do not include the dimensions of the steel canister (0.005-m wall thickness).

3.1. Pure radioactive products

If the product streams from the separations flowsheets are calcined and packaged, the composition of the radioactive materials will be the oxides. For the mixed product streams of 10.5% Cm_2O_3 in 89.5% Am_2O_3 (Table 2), the maximum radii $r_{\max}$ are 0.0114 m and 0.0094 m for storage in water and air, respectively. The density of the storage form does not significantly affect these values. For a product of 26% SrO in 74% Cs_2O (Table 2), the $r_{\max}$ are 0.040 m and 0.020 m for water and air storage, respectively, at theoretical density. Water storage at 70% theoretical density reduces the maximum radius to 0.026 m for Cs/Sr oxides because of the lowered thermal conductivity from porosity. The surface temperature for storage in air varies from 637 K for theoretically dense Am/Cm to 516 K for 70% porous Cs/Sr. That for storage in water is 322–331 K.

These values are comparable to those of typical nuclear fuel rods, where thin-rod fabrication technology is demonstrated. US light water reactor fuels are 0.0047–0.0064 m in radius depending on whether they are pressurized-water-reactor or boiling-water-reactor fuel. Mixed-oxide fuel (MOX) from the MELOX plant (Marcoule site, France) is 0.00475 m in radius [8]. Experimental Breeder Reactor II (EBR-II) fuel pins were 0.00183 m in radius [8]. Certainly, there is industry experience in fabricating the desired storage form dimensions since the LWR and MOX fuel dimensions are roughly a factor of four smaller than the Cs/Sr oxides storage forms and approximately half the radius of the Am/Cm oxides. However, LWR fuel is sintered from low-level radioactive material and EBR-II elements were cast

[2] Ninety percentage of the melting point was assumed to be an adequate factor of safety for this analysis. The authors realize that larger factors of safety may be necessary and use 90% as a starting point.

Table 2
Maximum radii for pure oxide storage forms at various porosities

Coolant		Am_2O_3/Cm_2O_3			Cs_2O/SrO		
		100%	80%	70%	100%	80%	70%
Air	r_{max}	0.0092	0.0094	0.0094	0.0205	0.0185	0.0174
	h_{rad}	27.4	24.6	23.1	23.1	19.5	17.8
	h_{conv}	9.92	9.93	9.93	8.61	8.75	8.79
	$T_{surface}$	637	605	587	587	540	516
Water	r_{max}	0.0114	0.0113	0.0112	0.0397	0.0294	0.0255
	h_{rad}	6.7	6.6	6.6	6.8	6.6	6.5
	h_{conv}	975	931	906	816	768	741
	$T_{surface}$	327	324	323	331	324	322

from molten metal; both operations ease processing. The MELOX MOX fuel is fabricated from blended powders and sintered in remote glovebox units. With modifications to shielding and cooling and additional checks for radiation damage to equipment, it appears that the MELOX technology is suitable for fabrication of the engineered product storage forms.

3.2. Fins

Finned canisters can help dissipate the heat. We assumed the fins extend 150% from the bare surface (measured radially from centerline), with a half-thickness of 0.25 mm and 1 mm and covering 20–40% of the total canister surface. At theoretical density, r_{max} for Cs/Sr oxide storage material in air increases 26–68% over a bare canister depending on the fin dimension and coverage (Table 3). The fins increase r_{max} by 15% for Am/Cm oxides. Storage in water is not benefited by fins due to the large natural convective heat transfer coefficients in water.

3.3. Coolant temperature excursion

If the ambient temperature rises considerably the heat transfer will be affected. Supposing the average air temperature is 473 K instead of the 363 K assumed in our previous analysis, the maximum radius of the theoretically dense Cs/Sr storage canister is reduced to 0.0172 m from 0.0205 m for 363 K ambient coolant and, for Am/Cm, to 0.00785 m from 0.0080 m for 363 K ambient coolant.

Table 3
Parameters for finned Cs/Sr oxide canisters (coverage refers to the percent of bare cylinder surface occupied by fins)

	$y_b = 0.25$ mm, coverage = 40%	$y_b = 1$ mm, coverage = 40%	$y_b = 1$ mm, coverage = 20%
r_{max}	0.0345	0.0292	0.0258
h_{rad}	12.16	16.22	18.92
h_{conv}	228	68	36
$T_{surface}$	417	491	531.68
Ω	0.31	0.31	0.31

3.4. Fuel age

The out-of-reactor time for nuclear fuels will vary from fuel assembly to assembly. The age may span 10–60 years. As the fuel ages intact, the cesium and strontium decay with an approximately 30-year half-life. Curium decays with an 18-year half-life (dominated by ^{244}Cm) but americium grows into the fuel as a result of ^{241}Pu decay. We investigated the effect of fuel age on the thermal load and heat transport of the resulting storage forms (Table 4). Cesium and strontium recovered from 10-year-old fuel has a thermal power of 0.18 W/g as oxides. Americium and curium has a thermal power of 0.29 W/g as oxides. In 60-year-old fuel the thermal power is 0.12 W/g for Cs/Sr oxides and 0.10 W/g for Am/Cm oxides. The resulting r_{max} for Cs/Sr oxides is 0.027 m and 0.051 m in air and water, respectively, and 0.015 m and 0.018 m, respectively, for Am/Cm oxides.

3.5. Diluted radioactive products

There are various reasons why the high-heat radionuclides would be diluted in non-radioactive materials. Those reasons include lowering the radionuclide concentration to meet Class C waste classification, reducing the heat source density, and stabilizing the radioactive material in a more durable composite.

We assume that Cs/Sr may be diluted in aluminosilicate resins (i.e., zeolite, pollucite, or feldspar) or glass

Table 4
r_{max} for 60-year-old PWR fuel (50 GWd/MT)

Coolant	Cs/Sr Ox	Am/Cm Ox
Air	0.027	0.015
Water	0.051	0.018

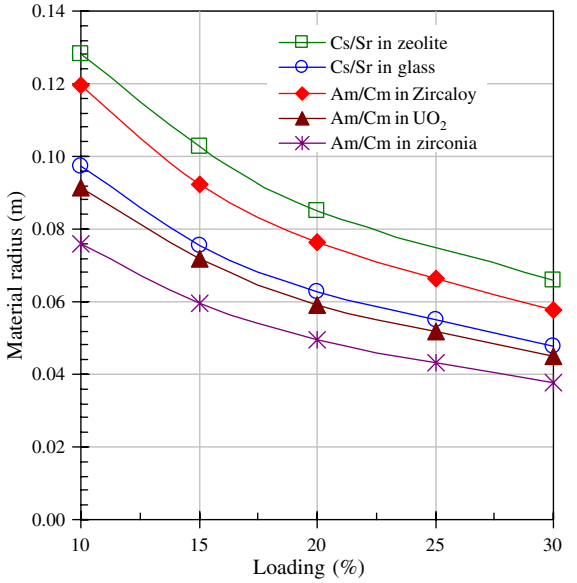

Fig. 4. r_{max} for Cs/Sr oxide and Am/Cm oxide diluted in various materials as a function of radioactive loading.

and Am/Cm oxides in sintered Zircaloy (as an example of a high k diluent), uranium dioxide, or zirconia (Fig. 4). We compare these values to the baseline r_{max} of 0.0092 m for Am/Cm oxides and 0.0205 m for Cs/Sr oxides. r_{max} for Cs/Sr oxides increases by about a factor of 3 in alumino-silicate and a factor of 2 in glass at 30% loading. That for Am/Cm oxides increases by a factor of 6.5 in Zircaloy, 5 in UO_2, and 4 in zirconia at 30% loading.

3.6. Pure Cm product

Because Cm and Am have different strategic paths in the transmutation cycle there is an advantage to isolating them from each other. This would require short-term decay storage of the Cm product to concentrate the plutonium daughters. This lag period is envisioned to be less than 10 years but it may be as long as 50 years. The specific thermal power of Cm_2O_3 is very high (2.34 W/g for reference fuel) but the melting point is also high (2280 K). The resulting r_{max} for theoretically dense Cm_2O_3 is 0.0061 m, significantly smaller than for the reference Am/Cm oxides (0.0092 m); however, the higher k for Cm_2O_3 (2.0 W/m/K) reduces the thermal gradient across the storage form, raising the surface temperature to 1830 K. Such high-temperature forms are difficult to handle and containerize. If we restrict the surface temperature to 700 K, then an 80% dense form has a smaller radius, $r_{max} = 0.0022$ m, a reduction of more than a factor of 4 from the reference Am/Cm oxide.

To increase r_{max} we can dilute the Cm_2O_3. High-burnup aluminum-based dispersion fuels have been fabricated for research and test reactors operating at relatively low temperatures [9]. The aluminum matrix provides efficient thermal transport ($k = 190$–300 W/m/K) but the solidus temperature is relatively low ($T_{solidus} = 786$ K). We considered 10%, 30%, and 50% loading of Cm_2O_3 in aluminum, where r_{max} is 0.0085 m, 0.0041 m, and 0.0030 m, respectively for a theoretically dense form.

Similarly to Am/Cm oxides, we consider dilution of Cm_2O_3 in Zircaloy. At 10% loading and 80% theoretical density, r_{max} is 0.019 m, but the surface temperature is 1050 K. Limiting the surface temperature to 700 K reduces r_{max} to 0.010 m.

Therefore, the pure Cm product presents a rather unique problem. In the pure form, the poor thermal conductivity limits the r_{max} to 0.0022 m. Such a thin rod has been fabricated routinely for EBR-II, but not with oxide powders and certainly not with a highly radioactive source. The dilution of the material in a high thermally conductive material does not provide the expected benefit of a larger radius. This is due to the resulting high surface temperature, which makes handling difficult. We must reduce the thermal power of the radioactive material and simultaneously limit surface temperatures. Thus, either of two scenarios seems plausible. First, we dilute the Cm in a refractory material. One candidate is depleted uranium oxide. At 80% dense and 700 K maximum surface temperature, Cm_2O_3 mixed with UO_2 powder can be fabricated to 0.010 and 0.0049 m, for 10 and 30% Cm_2O_3 loading, respectively. Loading into zirconia (700 K surface temperature) produces identical values. These values are identical to those for the case of Cm_2O_3 in Zircaloy. The other scenario to avoid centerline melt is to fabricate thin plates such as those prepared for high-burnup Al-based nuclear fuels [10]. The powder metallurgical methods for these fuels may be appropriate for the thin dimensions required for an Al–Cm_2O_3 form, since Al-based fuel meat thicknesses were quite small – several millimeters in thickness. There is also a wealth of industry experience in fabricating fuel plates.

3.7. Sensitivity analysis

We completed a perturbation analysis to quantify the sensitivity of the centerline temperature to several model parameters, f_i (Fig. 5). We note that the centerline temperature is relatively sensitive to storage form radius, h_{total} in air, and k of the Cs/Sr oxide material. The values for h_{total} in air and k for Cs/Sr oxides are low, so small changes to these values can markedly affect thermal transport. A change in the radius or linear thermal power of 10% causes a 7% change in centerline temperature. Therefore, at 1000 K we would expect a 70 K swing in the centerline temperature. A similar change in h_{total} in air results in a 3.7–4.7% change in centerline temperature

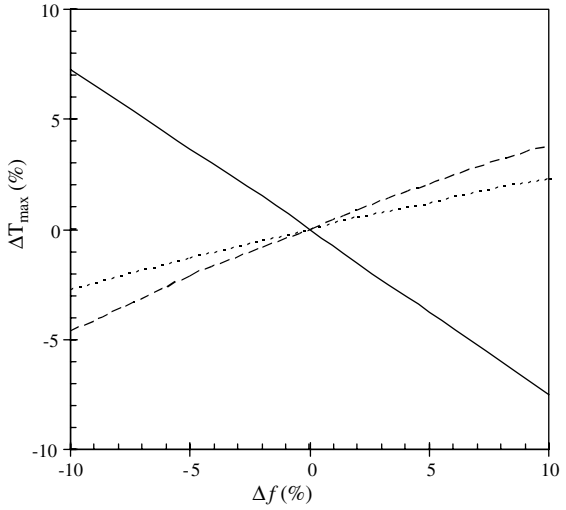

Fig. 5. Sensitivity analysis showing that the centerline temperature is a relatively strong function f of the h_{conv} in air (–––), $k_{mixture}$ (- - -), the radius of the storage form (line), and the linear thermal power (coincides with radius).

and 2.2–2.7% change for a perturbed k for the radioactive oxide material.

On the other hand, the centerline temperature is not sensitive to the h_{total} for water, k for the canister material (assumes a metal canister), and the convective heat transfer coefficient in the gap between the storage form and canister (data not shown). A 10% change in any of these parameters results in <1% change in centerline temperature.

4. Summary and conclusions

We describe an algorithm that calculates the temperature profile within high-heat radioactive storage forms under natural convective cooling. The model can describe mixed Am_2O_3/Cm_2O_3 products, Cs_2O/SrO products, and Cm_2O_3 products either in pure form or diluted in several potentially attractive materials. Different storage compositions can be easily input into the model. Porosity and imperfect thermal contact between the canister and storage material has been accounted.

Pure Am/Cm oxides are limited to canisters with radii equal to 0.0092 m if stored in air or 0.011 m if stored in water. The lower thermal power density of pure Cs/Sr oxides results in maximum radii of 0.020 m in air and 0.040 m in water. Porosity reduces the thermal transport efficiency of the Cs/Sr oxide significantly, reducing the maximum radii. Cooling fins increase cooling of the Cs/Sr oxide canisters more effectively than the Am/Cm oxide canisters but the added benefit is small and of little utility.

If the environmental stability of the oxides is considered too poor for temporary storage or we wish to modify the thermal transport properties of the storage products, we can dilute the radioactive oxides. Am/Cm oxide storage forms can be increased to 0.120 m in radius if loaded to 10% in a high k matrix such as Zircaloy. Cs/Sr oxide storage forms can be increased to 0.128 m in alumino-silicates at 10% loading.

If the fuel separation processes generate a pure curium product stream then the storage material will be significantly smaller (0.0022 m for pure Cm_2O_3). This is comparable to the EBR-II fuel dimensions. However, molten metal casting, the process used for EBR-II, will not be used to fabricate the curium oxide products, thereby complicating potential unit operations. Even 10% Cm_2O_3 in Zircaloy or UO_2 limits the radius to 0.010 m due to the prohibitively high surface temperatures. Dilution of a pure curium product appears to be necessary, although thin plates are an attractive option to thin rods.

Perturbation analysis shows that the model is relatively sensitive to changes in the convective heat transport coefficient if air is the coolant, and to the thermal conductivity of the storage form mixture, the radius of the storage form, and the linear thermal power. We therefore stress the need to experimentally measure centerline temperatures of fuel surrogates and validate the model described here.

At this point, we can describe potential facility dimensions based on the engineered product dimensions and thermal power. In Part II of this study, we explore proposed storage facility concepts and calculate the relative sizes of these facilities.

Acknowledgements

The valuable guidance provided by Drs James Laidler and George Vandegrift are much appreciated. Work is supported by the US Department of Energy, Office of Nuclear Energy, Science and Technology, under Contract No. W-31-109-ENG-38.

References

[1] US Department of Energy, Report to Congress on Advanced Fuel Cycle Initiative: The Future Path for Advanced Spent Fuel Treatment and Transmutation Research, Office of Science and Technology, January 2003.
[2] R.B. Bird, W.E. Stewart, E.N. Lightfoot, Transport Phenomena, John Wiley, New York, 1960, p. 412.
[3] H. Kato, N. Nishiwaki, M. Hirata, Int. J. Heat Mass Transfer 11 (7) (1968) 1117.
[4] D.Q. Kern, Process Heat Transfer, McGraw-Hill, New York, NY, 1950, p. 77, 512.
[5] R. Krupiczka, Int. Chem. Eng. 7 (1967) 122.

[6] Y. Benveniste, J. Appl. Phys. 61 (8) (1987) 15.
[7] C. Richter, H.J. Viljoen, N.F.J. van Rensburg, J. Appl. Phys. 93 (5) (2003) 2663.
[8] Dr. James. J. Laidler, Argonne National Laboratory, Personal communication, July 2004.
[9] A.G. Samoilov, A.I. Kashtanov, V.S. Volkov, Dispersion-Fuel Nuclear Reactor Elements, translated from Russian, Israel Program for Scientific Translations, Jerusalem, 1968.
[10] G.L. Hofman, J.L. Snelgrove, Mater. Sci. Technol. 10A (1994) 45.